Tunnable Substrate Wettability by Thin Water Layer

Felipe Jiménez-Ángeles[†] and Abbas Firoozabadi[*,†,‡]

Reservoir Engineering Research Institute, Palo Alto, CA 94301, USA, and Department of Chemical and Environmental Engineering, Yale University, New Haven, CT 06510, USA

E-mail: abbas.firoozabadi@yale.edu

Phone: +1 (650)326-9172. Fax: +1 (650) 472-9285

Supporting Information

Contact angle setup construction

The droplet is built (see Figure S1a) by placing 2340 n-decane molecules in a prismatic box of approximately 18 nm × 6.5 nm × 7.0 nm forming five layers, each layer is made of 468 molecules. 120 surfactant molecules are placed inside the hydrocarbon droplet between the layers of n-decane molecules. Aqueous solutions are prepared separately in three prismatic boxes, two of 18.6 nm × 6.1 nm × 7 nm and a third one of 18.5 nm × 18.7 nm × 5 nm, respectively. A 2-ns MD simulation is performed at $P = 200$ bar and $T = 298$ K in 3D periodic boundary conditions. The system evolves to a cylindrical droplet (see Figure S1a).

To take into account the hydration of the substrate, pre-equilibration of the surface is carried out by placing the substrate next to an aqueous solution at salt concentration ρ_s and equilibrated by means of a 3-ns molecular dynamics simulation (see Figure S1b). The ions

---
[*]To whom correspondence should be addressed
[†]Reservoir Engineering Research Institute
[‡]Yale University

and water molecules above a distance z_h from the substrate are removed and molecules within $z < z_h$ are kept as part of the hydrated substrate; z is measured from the outermost layer of oxygen atoms from the substrate. The value of z_h is established based on the perpendicular density profiles and it varies from $z_h = 0.8$ nm at 0 wt% NaCl to $z_h = 1.0$ nm at 6.3 wt% NaCl. Details of the pre-equilibration simulations are given elsewhere.[1] The composition of the simulated setups is given in Table I.
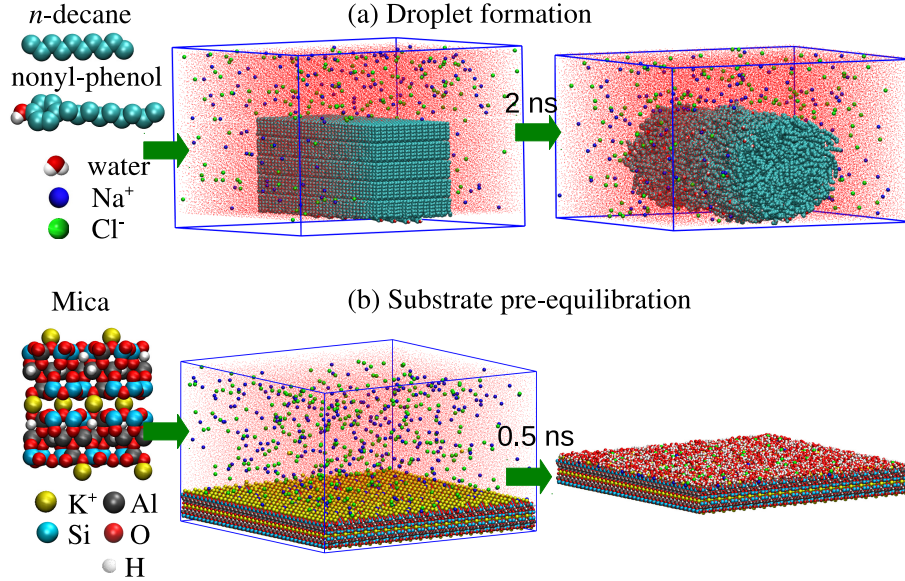

Figure S1: Graphical representation of the setup creation steps; (a) droplet formation, and (b) substrate pre-equilibration. The color code is the same as in Figure 1.

Contact angle calculation method

We use the density profiles of n-decane $\rho_d(y, z)$ to define the droplet shape. The density contour profiles in the interfacial region ($\rho_d(y, z) = 0.5\rho_b$) are circular and concentric. The profiles are fitted by a circle given by $(y - y_0)^2 + (z - z_0)^2 = R^2$; y_0 and z_0 are the circle center coordinates and R is the circle radius. Figure S2 shows the bottom part of the droplet density contour profile at 0, 1.1, and 3.3 NaCl wt% from molecular dynamics simulations and the fitted circle. The contact angle θ is formed by: 1) the vertical line passing through the circle's center, and 2) the line connecting the circle's center and the intersection point of the droplet profile and the horizontal contact plane at (y_c, z_c) (see Figure S2). The contact

plane is defined where the droplet profile deviates from circular shape; it is different at each salt concentration because the thickness of the water layer may depend on the salt concentration. The contact angle is obtained by $\tan\theta = (y_c - y_0)/(z_c - z_0)$. The accuracy of the contour plot is ± 0.045 nm and ± 0.04 nm in y and z directions, respectively, which gives a contact angle error of about $\pm 0.3°$. The thickness of the fluid-fluid interface defined between $\rho_d(y, z) = 0.8\rho_b$ and $0.2\rho_b$ is about 0.45 nm thick. This thickness is for the region outside the confinement.
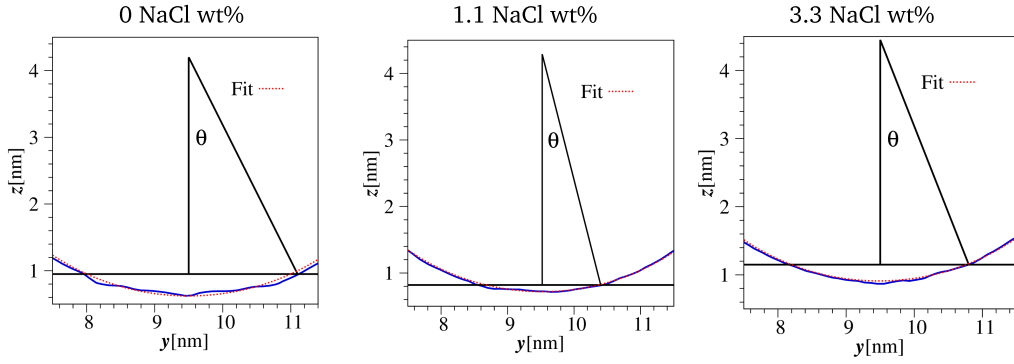

Figure S2: Closeup view of the bottom part of the droplet profile $\rho_d(y, z) = 0.5\rho_b$ at $\rho_s = 0$, 1.1, and 3.3 wt% NaCl . The contact angle θ is obtained from a fitted circle (red-dotted line) and its intersection at horizontal contact plane.

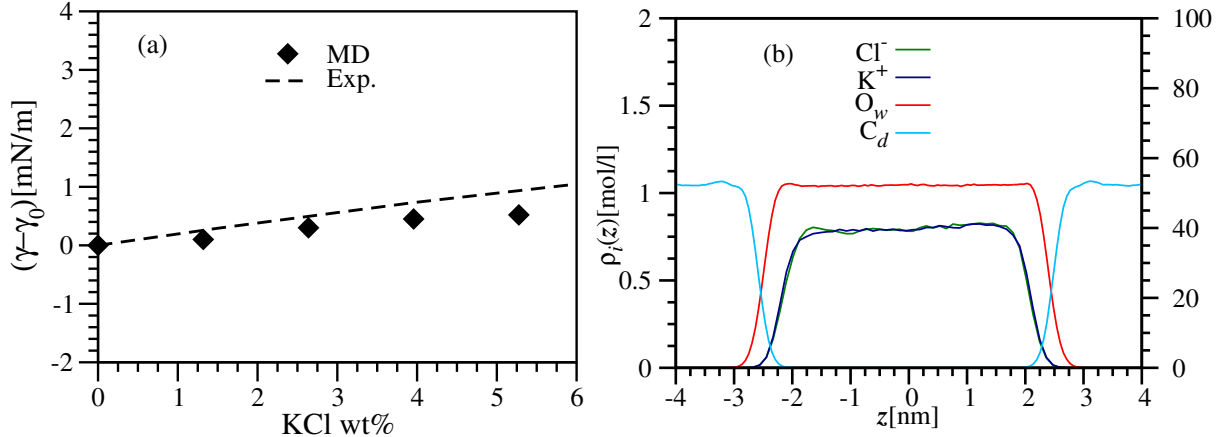**Fluid-fluid interface with KCl and KI**

Figure S3: n-decane-KCl solution interface. (a) Interfacial tension difference $(\gamma - \gamma_0)$ as a function of the KCl concentration in wt% ($P_z = 1$ bar and $T = 293$ K). Black diamonds are the results from MD simulations and the dashed line represents the measured interfacial tension.[2] The interfacial tension at zero salt concentration from MD simulations in n-decane is $\gamma_0 = 49.05$ mN/m; the experimental value in n-dodecane is $\gamma_0 = 52.81$ mN/m. The difference between the experimental interfacial tension of n-dodecane and n-decane is about 0.1 mN/m.[2] (b) Density profiles of K^+ and Cl^- ions, water-oxygen atom (O_w), and n-decane carbon atoms (C_d) in the n-decane-electrolyte solution interface at $\rho_s = 5.3$ KCl wt%. The left scale is for the ions and the right scale is for water-oxygen atoms and n-decane.

Figure S3a portrays the linear difference of the interfacial tension $(\gamma - \gamma_0)$ in n-decane-electrolyte solution as a function of the KCl concentration; the results from MD simulations are in agreement with the experimental measurements. The density profiles of the species in the n-decane-electrolyte solution interface are presented in Figure S3b at $\rho_s = 5.3$ KCl wt%. The K^+ and Cl^- density profiles show that the ions are outside the interface.

The interfacial tension difference $(\gamma - \gamma_0)$ of the n-decane-electrolyte solution as a function of the KI concentration is shown in Figure S4a. The results from MD simulations and the experimental measurements show that the interfacial tension is slightly less than γ_0 and stay nearly constant as a function of the KI concentration. The density profiles of the species in the n-decane-electrolyte solution interface are presented in Figure S4b at $\rho_s = 8.8$ KCl wt%. The density profiles show that ions are not equally distributed at the interface; I^- ions penetrate deeper into the interface than K^+ ions. The uneven ionic distribution at the interface produces a small decrease of the interfacial tension. Our results are different

from the prediction of a modified Poisson-Boltzmann theory where the ions I$^-$ are strongly adsorbed at the oil-water interface.[3]
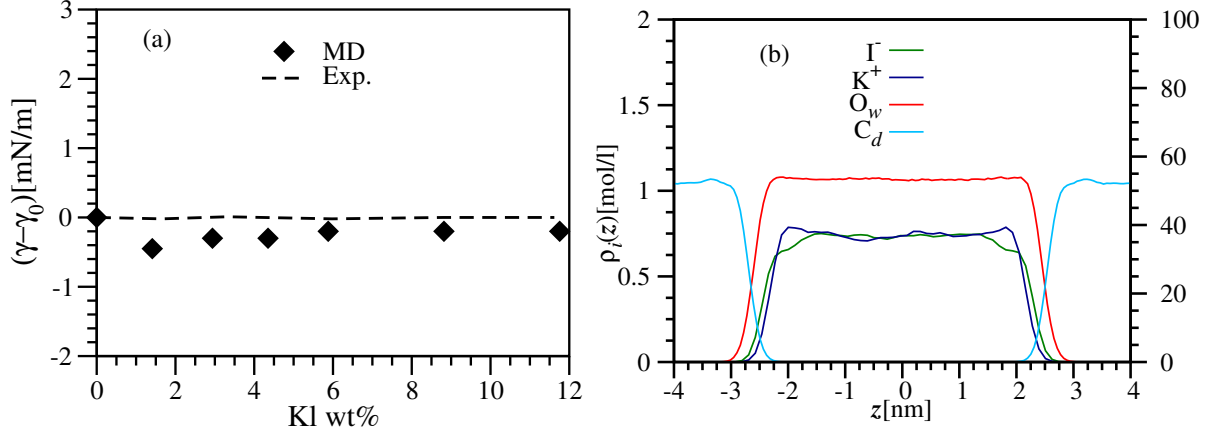

Figure S4: n-decane-KI solution interface. (a) Interfacial tension difference $(\gamma - \gamma_0)$ as a function of KI concentration in wt% ($P_z = 1$ bar and $T = 293$ K). Black diamonds are the results from MD simulations and the dashed line represents the measured interfacial tension in n-dodecane.[2] The difference between the experimental interfacial tension of n-dodecane and n-decane is about 0.1 mN/m.[2] The interfacial tension at zero salt concentration from MD simulations in n-decane is $\gamma_0 = 49.05$ mN/m; the experimental value in n-dodecane is $\gamma_0 = 52.81$ mN/m. (b) Density profiles of K$^+$ and I$^-$ ions, water-oxygen atom (O$_w$), and n-decane carbon atoms (C$_d$) in the n-decane-electrolyte solution interface at $\rho_s = 8.8$ KI wt%. The left scale is for the ions and the right scale is for water-oxygen atoms and n-decane.

Thin liquid layer at 0.1, 1.1 and 6.2 NaCl wt%:

The reduced density profiles and snapshots of the liquid layer under the droplet at 0.15, 1.9, and 6.3 NaCl wt% are shown in Figures S5, S6, and S7, respectively. At the three salt concentrations the density profile of water oxygen shows a sharp peak at $z \approx 0.26$ nm and a hump at $z \approx 0.20$ nm. Depending on the salt concentration other peaks are observed at higher z. The water density profile drops monotonically to zero towards the oil droplet. The water layer thickness is 0.5, 0.76, and 1.1 nm at 0.15, 1.9, and 6.3 NaCl wt%, respectively. The reduced density profile of n-decane increases from zero in the water layer to a bulk value in the oil droplet. The reduced density profile of n-decane changes as the salt concentration increases because of the increase of the water layer thickness.

The surfactant head density profiles in the thin liquid layer are centered at $z = 0.8$, 1, and 1.5 nm at 0.15, 1.9, and 6.3 NaCl wt%, respectively (Figures S5, S6, and S7). The center of the distribution reflects the water layer thickness. The interface at the bottom of the droplet is narrower (in the y-direction) at 1.9 NaCl wt% than at 0.15 and 6.3 NaCl wt%. As discussed in the text, the width of the rugged interface is related to the contact angle.

The Na$^+$ ions adsorbed on the substrate give rise to a sharp peak at $z \approx 0.2$ nm in the reduced density profiles shown in Figures S5, S6, and S7. At 1.9 NaCl wt%, Na$^+$ ions are nearly depleted from the middle region under the droplet and are found only at the lateral entries of the water layer. At 6.3 NaCl wt%, Na$^+$ ions are found in the confined liquid layer which is seen in the reduced density profile as a secondary peak at $z \approx 0.48$ nm. The Cl$^-$ reduced density profiles at 1.9 and 6.3 NaCl wt% (Figures S6 and S7, respectively) exhibit a peak at $z \approx 0.4$ nm and decrease to zero towards the oil droplet. Cl$^-$ ions compensate the charge of the adsorbed Na$^+$ ions. At 6.3 NaCl wt%, Cl$^-$ ions are observed at the middle region of the liquid layer whereas at 1.9 NaCl wt% Cl$^-$ ions are only found at the lateral entries of the liquid layer. At 0.15 NaCl wt%, Cl$^-$ ions are not found close to the confined liquid layer region; the Cl$^-$ density profile is zero.
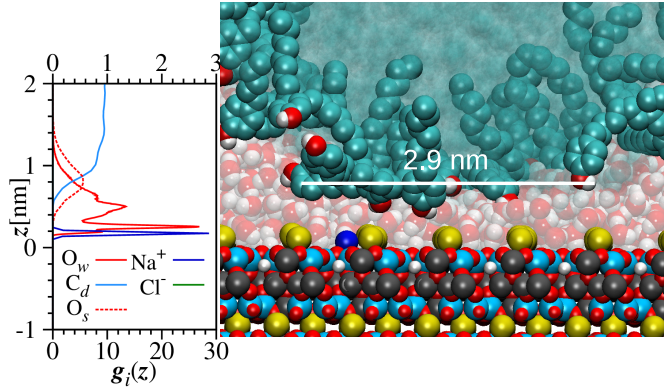
Figure S5: Left: Reduced density profiles of ions (Na^+ and Cl^-), water (O_w), n-decane (C_d), and the surfactant head oxygen (O_s) in the region between the droplet and the substrate at 0.15 wt% NaCl. Horizontal top scale is for O_w, C_d, and O_s whereas the bottom scale is for Na^+ and Cl^-. Right: Snapshot showing the ions, water, and n-decane molecules at the bottom part of the droplet. The region occupied by n-decane molecules is colored transparent-cyan whereas water molecules are semitransparent and in the background; the color code is the same as in Figure 1.
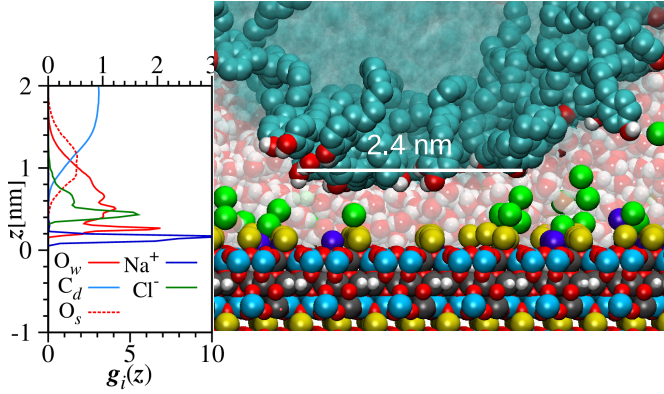

Figure S6: Left: Reduced density profiles of ions (Na^+ and Cl^-), water (O_w), n-decane (C_d), and the surfactant head oxygen (O_s) in the region between the droplet and the substrate at 1.9 wt% NaCl. Horizontal top scale is for O_w, C_d, and O_s whereas the bottom scale is for Na^+ and Cl^-. Right: Snapshot showing the ions, water, and n-decane molecules at the bottom part of the droplet. The region occupied by n-decane molecules is colored transparent-cyan whereas water molecules are semitransparent and in the background; the color code is the same as in Figure 1.
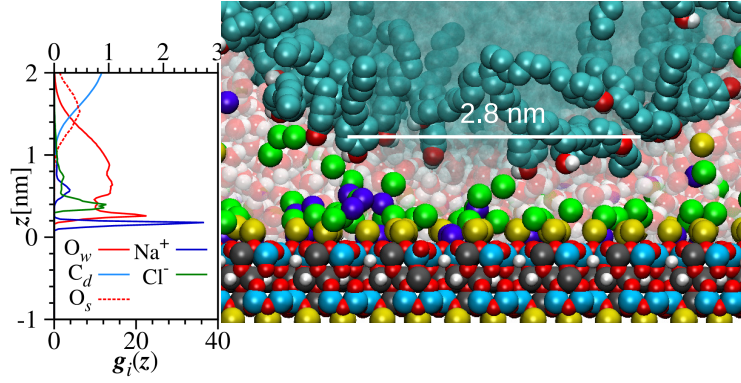
Figure S7: Left: Reduced density profiles of ions (Na^+ and Cl^-), water (O_w), n-decane (C_d), and the surfactant head (O_s) in the region between the droplet and the substrate at 6.3 wt% NaCl. Horizontal top scale is for O_w, C_d, and O_s whereas the bottom scale is for Na^+ and Cl^-. Right: Snapshot showing the ions, water, and n-decane molecules at the bottom part of the droplet. The region occupied by n-decane molecules is colored transparent-cyan whereas water molecules are semitransparent and in the background; the color code is the same as in Figure 1.

Ionic adsorption as a function of salt concentration

The reduced density profiles of Na$^+$ and Cl$^-$ ions in the region under the complex oil droplet are presented in Figures S8a and S8b, respectively, as a function of the perpendicular distance to the substrate and at different salt concentrations. The reduced density profiles of Na$^+$ and Cl$^-$ ions in the region under the model oil droplet (n-decane) are presented in Figures S9a and S9b, respectively. Na$^+$ and Cl$^-$ adsorption at the region under complex oil droplet exhibits a non-monotonic behavior. The minimum of Na$^+$ adsorption under the complex oil droplet is observed at 1.1 wt% NaCl and is more pronounced in the complex oil droplet. At 0.15 wt% NaCl, Cl$^-$ ion density profile is zero under the complex oil droplet.
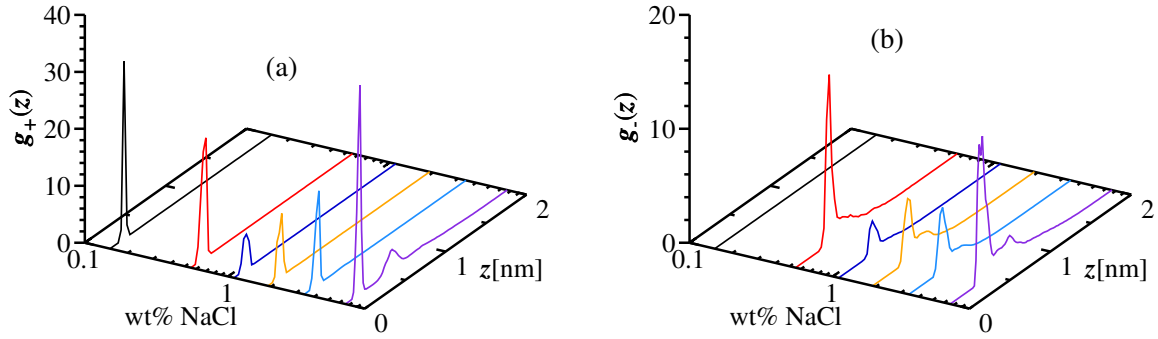

Figure S8: The reduced density profiles of (a) Na$^+$ and (b) Cl$^-$ ions in the region between the complex oil droplet and the substrate at 0.15 (black), 0.55 (red), 1.1 (blue), 1.9 (yellow), 3.3 (light blue), and 6.3 (purple) wt% NaCl.
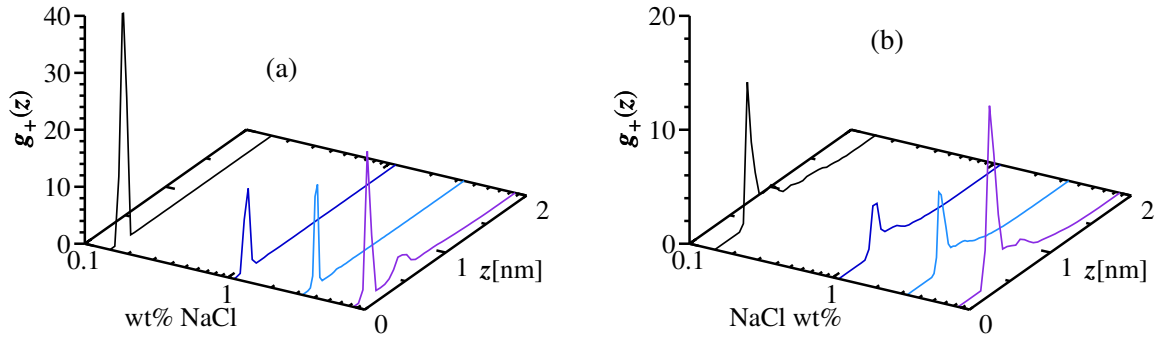
Figure S9: The reduced density profiles of (a) Na^+ and (b) Cl^- ions in the region between the model oil droplet and the substrate at 0.15 (black line), 1.1 (blue), 3.3 (light blue), and 7.7 (purple) wt% NaCl.

Simulation Parameters

Table S1: Lennard-Jones parameters and charge of ions in the solution[4]

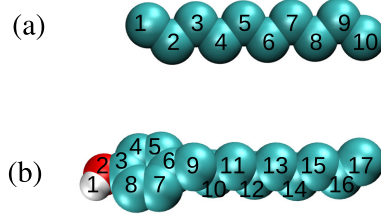| Atom	$q[e]$	$\sigma[\text{nm}]$	$\epsilon[\text{kJ/mol}]$
Na^+	1	0.333	1.16×10^{-2}
K^-	1	0.365	8.36×10^{-1}
Cl^-	-1	0.441	4.93×10^{-1}
I^+	-1	0.54	1.92×10^{-2}

Figure S10: (a) n-decane and (b) nonylphenol molecules; the atom indices used to assign the force field parameters in Tables S1 to S3 are shown.

Table S2: Lennard-Jones parameters of beads forming n-decane. Indices are assigned according to Figure S10a.

Index	Atom	$q[e]$	$\sigma[\text{nm}]$	$\epsilon[\text{kJ/mol}]$
1 and 10	CH_3	0	0.390	7.32×10^{-1}
2 to 9	CH_2	0	0.390	4.93×10^{-1}

The torsion potential energy in the n-decane molecule is modeled by means of the Fourier function $V_F(\phi) = 1/2[C_1(1 + \cos(\phi)) - C_2(1 + \cos(2\phi)) + C_3(1 + \cos(3\phi)) - C_4(1 + \cos(4\phi))]$; ϕ is the dihedral angle. The coefficients are given in Table S4.[5]

Table S3: The equilibrium bond distance (b_0) between pairs of first neighbors and the equilibrium bending angle (θ_0) in triplets of neighboring atoms in the n-decane molecule.[5]

Molecule	b_0[nm]	θ_0[°]
n-decane	0.153	114

Table S4: C_n torsion parameters in quadruplets of neighboring atoms of n-decane

Molecule	C_1[kJ/mol]	C_2[kJ/mol]	C_3[kJ/mol]	C_4[kJ/mol]
n-decane	5.90	-1.13	13.15	0

Table S5: Lennard-Jones parameters of beads forming the surfactant molecule (nonylphenol).[5,6] Indices are assigned according to Figure S10b.

index	Atom	q[e]	σ[nm]	ϵ[kJ/mol]
1	H	0.435	0.00	0.00
2	O	-0.585	0.307	0.711
3	CH	0.150	0.375	0.460
4 to 8	CH	0.00	0.375	0.460
9 to 16	CH_2	0.00	0.390	4.93×10^{-1}
17	CH_3	0.00	0.370	7.32×10^{-1}

Table S6: Bond distance b_0 between pairs of first neighbors. Indices are assigned according to Figure S10b.

Molecule	Indices	b_0[nm]
Nonylphenol	1,2	0.095
Nonylphenol	2 to 8	0.139
Nonylphenol	3,9; 9 to 17	0.153

Table S7: Bending equilibrium θ_0 angle in triplets of neighboring atoms in the surfactant molecule. Indices are asigned according to Figure S10b.

Molecule	Indices	θ_0[°]
Nonylphenol	1,2,3	114
Nonylphenol	2,3,4; 2,3,8	120
Nonylphenol	3 to 8	120
Nonylphenol	6,9,10; 9 to 17	114

Dihedral angles of the atoms in the aromatic ring of the head are described by the Ryckaert-Bellemans function[7] $V_{RB}(\phi) = \sum (-1)^n F_n (\cos(\phi))^n$; the F_n coefficients are given in Table S8.

Table S8: F_n torsion parameters in quadruplets in the surfactant head (atoms 3 to 8, see Figure S10b).

Molecule	F_1[kJ/mol]	F_2[kJ/mol]	F_3[kJ/mol]	F_4[kJ/mol]	F_5[kJ/mol]
Nonylphenol	30.33	0.00	-30.33	0.00	0.00

Dihedral angles in the OH group-aromatic ring and in the head-tail junctions are described by $V_d(\phi) = k_\phi [1 + \cos(2\phi - \phi_0)]$; the atoms indices and the constants are given in Table S9.

Table S9: Dihedral angle parameters in quadruplets in the OH group-aromatic ring and in the head-tail junctions.

Indices	k_ϕ(kJ/mol/)	$\phi_0[^\circ]$
1,2,3,4	4.6	180
2,3,4,5	4.6	180
5,6,9,10	1.1	0.0

Additional torsion angles in the tail of nonylphenol (atoms 9 to 17) are described by the same function and parameters as in n-decane (Table S4).

References

(1) Jiménez-Ángeles, F.; Firoozabadi, A. Contact Angle, Liquid Film, Liquid-Liquid and Liquid-Solid Interfaces in Model Oil-Brine-Substrate Systems. *J. Phys. Chem. C* **2016**, *120*, 11910–19917.

(2) Aveyard, R.; Saleem, S. M. Interfacial Tensions at Alkane-Aqueous Electrolyte Interfaces. *J. Chem. Soc., Faraday Trans. 1* **1976**, *72*, 1609–1617.

(3) dos Santos, A. P.; Levin, Y. Ions at the Wateroil Interface: Interfacial Tension of Electrolyte Solutions. *Langmuir* **2012**, *28*, 1304–1308.

(4) Jorgensen, W. L. In *The Encyclopedia of Computational Chemistry*; Schleyer, e. a., P. v. R., Ed.; John Wiley & Sons: Dordrecht, 1998; Vol. 3; Chapter OPLS Force Fields.

(5) Martin, M. G.; Siepmann, J. I. Transferable Potentials for Phase Equilibria. 1. United-Atom Description of n-Alkanes. *J. Phys. Chem. B* **1998**, *102*, 2569–2577.

(6) Jorgensen, W. L.; Tirado-Rives, J. The OPLS [Optimized Potentials for Liquid Simulations] Potential Functions for Proteins, Energy Minimizations for Crystals of Cyclic Peptides and Crambin. *J. Am. Chem. Soc.* **1988**, *110*, 1657–1666.

(7) Ryckaert, J.-P.; Bellemans, A. Molecular Dynamics of Liquid n-butane Near its Boiling Point. *Chem. Phys. Lett.* **1975**, *30*, 123–125.